

Nonlinear parametric resonance of relativistic electrons with a linearly polarized laser pulse in a plasma channel

T. W. Huang,^{1,2} C. T. Zhou,^{1,2,3,*} A.P.L. Robinson,^{4,†} B. Qiao,^{2,‡}
A. V. Arefiev,⁵ P.A. Norreys,^{4,6} X. T. He,^{2,3} and S. C. Ruan¹

¹*College of Optoelectronic Engineering, Shenzhen University, Shenzhen 518060, People's Republic of China*

²*HEDPS, Center for Applied Physics and Technology and School of Physics,
Peking University, Beijing 100871, People's Republic of China*

³*Institute of Applied Physics and Computational Mathematics, Beijing 100094, People's Republic of China*

⁴*Central Laser Facility, STFC Rutherford-Appleton Laboratory, Didcot, OX11 0QX, United Kingdom*

⁵*Institute for Fusion Studies, The University of Texas, Austin, Texas 78712, USA*

⁶*Clarendon Laboratory, Department of Physics, University of Oxford,
Parks Road, Oxford, OX1 3PU, United Kingdom*

(Dated: November 8, 2016)

The direct laser-acceleration mechanism, nonlinear parametric resonance, of relativistic electrons in a linearly-polarized laser-produced plasma channel is examined by a self-consistent model including the relativistic laser dispersion in plasmas. Nonlinear parametric resonance can be excited and the oscillation amplitude of electrons grows exponentially when the betatron frequency of electron motion varies roughly twice the natural frequency of the oscillator. It is shown analytically that the region of parametric resonance is defined by the self-similar parameter $\frac{n_e}{n_c a_0}$. The width of this region decreases with $\frac{n_e}{n_c a_0}$, but the energy gain and oscillation amplitude increases. In this regime, the electron transverse momentum grows faster than that in the linear classical resonance regime.

PACS numbers: 52.38.Kd, 41.75.Jv, 52.38.Ph, 52.59.-f

I. INTRODUCTION

The dynamics of electron acceleration in the interaction of ultra-intense laser pulses with under-dense plasmas have attracted great attention because of its fundamental interest in laser plasma physics as well as its relation to many potential applications, ranging from particle acceleration [1–5], and positron production [6], to generation of X-rays and Gamma-rays [7–15]. Laser-based radiation sources could be highly compact and cost-effective compared with the traditional light sources. The characteristics of the radiation are determined by the dynamics of betatron oscillation of electrons in the laser-produced plasma channel, in which the self-generated magnetic and electrostatic fields play the role of the wiggler. Especially it is noted that both the radiated photon energy and number are proportional to the transverse betatron strength parameter, which is proportional to the oscillation amplitude of betatron motion and the electron energy. In order to obtain a radiation source with high photon flux and high photon energy, both the energy and betatron amplitude of the electrons should be amplified as much as possible in the plasma channel.

One promising way to enhance both the energy and transverse amplitude of the electron is the betatron resonance or the direct laser acceleration, which has been widely investigated both theoretically and experimentally [16–22], and it occurs when the oscillation frequency of

the electron in the fields of the plasma channel is equal to the laser frequency witnessed by the electron. The laser energy will be largely absorbed by the electrons when the resonance condition is satisfied, leading to the generation of “superponderomotive” electrons [23]. Meanwhile, the transverse betatron amplitude is also enhanced and high brightness synchrotron X-rays are produced [12–15]. However, in nature this kind of resonance is still a linear process, which indicates that the energy and oscillation amplitude of the electron grow linearly with time [21, 24].

For electrons interacted with a linearly polarized laser pulse in a plasma channel, the betatron motion of the electron can be described in the form of a parametric oscillator, whose betatron frequency oscillates in time. In this case, parametric resonance can be excited and the oscillation amplitude of electrons grows exponentially when the betatron frequency varies roughly twice the natural frequency of the oscillator [24, 25]. It is quite different from the classical betatron resonance because it manifests the instability phenomenon. This scheme was first proposed and investigated by Arefiev, et al [25]. It was revealed that the parametric resonance is a threshold phenomenon and multiplication of the laser intensity and plasma density should be larger than a threshold value in order to excite the parametric resonance. However, in previous works the electron response on the laser pulse was neglected at a sufficient low plasma density. To give an upper limit of the plasma density, a self-consistent model including the plasma response on the laser pulse should be considered. In addition, it had been shown that the wave dispersion in plasmas would play an important role on electron dynamics [26].

In this work, the possibility of electron acceleration in

* zcangtao@iapcm.ac.cn

† alex.robinson@stfc.ac.uk

‡ bqiao@pku.edu.cn

the laser produced plasma channel via a nonlinear parametric resonance process is re-examined by considering a three-dimensional model that self-consistently incorporates the relativistic laser dispersion in underdense plasmas. Based on this model, the region of phase space over which parametric resonance occurs and the electron oscillations grow nonlinearly in time is given. In particular it is shown that the region of parametric resonance can be characterized by a single parameter $\frac{n_e}{n_e a_0}$. This controls both the energy gain and the width of resonance region. Exploiting parametric resonance in direct laser acceleration therefore requires control of this parameter. Using a small value of $\frac{n_e}{n_e a_0}$ leads to the greatest enhancement of both the electron energies and transverse momenta, at the expense of restricting the width of resonance region. An upper limit value of $\frac{n_e}{n_e a_0}$ is also given to observe the efficient parametric resonance process.

The paper is organized as follows. In Sec. II, a self-consistent physical model that incorporates the laser dispersion relation is introduced and theoretical analyses on the parametric resonance behavior are also given based on this physical model. In Sec. III, numerical simulations based on the physical model are conducted to verify the theoretical predictions in Sec. II. Particularly, the parameter dependency of parametric resonance process on different laser and plasma parameters are studied. In Sec. IV, the effects of finite size laser beam and the trade-off problem on parametric resonance are discussed. The summary is given in the final section.

II. PHYSICAL MODEL AND THEORETICAL ANALYSES

In order to illustrate the parametric resonance behavior of electrons in a plasma channel, the dynamics of a single electron interacting with the self-generated channel fields and a linearly polarized laser pulse are considered. For a linearly polarized plane wave propagating along the z direction, its transverse electromagnetic fields are $E_{Lx} = E_0 \cos(\phi)$ and $B_{Ly} = E_{Lx}/v_{ph}$, where $\phi = kz - \omega_0 t$, ω_0 is the laser frequency, k is the wave number, $v_{ph} = \omega_0/k$ is the phase velocity, and E_0 denotes the amplitude of the laser field. The transverse self-generated fields are assumed to be E_{Sx} , E_{Sy} , B_{Sx} , and B_{Sy} . After some algebra, one can obtain the following four coupled equations of motion for the electron:

$$\frac{dp_x}{dt} = -e\eta E_0 \cos(\phi) - eE_{Sx} + ev_z B_{Sy}, \quad (1)$$

$$\frac{dp_y}{dt} = -eE_{Sy} - ev_z B_{Sx}, \quad (2)$$

$$\frac{dp_z}{dt} = -ev_x E_0 \cos(\phi)/v_{ph} - ev_x B_{Sy} + ev_y B_{Sx}, \quad (3)$$

$$m_e c^2 \frac{d\gamma}{dt} = -ev_x E_0 \cos(\phi) - ev_x E_{Sx} - ev_y E_{Sy}, \quad (4)$$

where $\eta = 1 - v_z/v_{ph}$, m_e is the rest electron mass, c is the light speed in vacuum, and $\gamma =$

$\sqrt{1 + (\frac{p_x}{m_e c})^2 + (\frac{p_y}{m_e c})^2 + (\frac{p_z}{m_e c})^2}$ is the Lorentz factor of the electron. The plasma response to the laser field is incorporated in the laser dispersion relation. It will be shown later that the phase velocity of the laser pulse propagating into the plasmas would affect the electron dynamics significantly.

The above equations can well describe the electron acceleration process in the plasma channel [14, 15, 19–23, 25]. Based on this simple model, one can clearly understand the physical mechanisms of electron acceleration and the dependence of electron acceleration on different laser and plasma parameters. For a cylindrically symmetric plasma channel, the electron density is assumed to be $f n_e$, then the static fields of the plasma channel can be expressed as $E_{Sx} = (1 - f)m_e \omega_p^2 x/2e$, $E_{Sy} = (1 - f)m_e \omega_p^2 y/2e$, $B_{Sx} = f m_e \omega_p^2 v_z y/2c^2 e$, and $B_{Sy} = -f m_e \omega_p^2 v_z x/2c^2 e$. Here $0 \leq f \leq 1$, $\omega_p = \sqrt{\frac{n_e e^2}{\epsilon_0 m_e}}$ is the plasma frequency, n_e is the plasma density, and ϵ_0 is the vacuum permittivity. In previous works, the value of f is usually taken as $1/2$ [27, 28]. In our case, it will be shown later that the exact value of f does not affect the electron dynamics. It is noted that the transverse static fields vary linearly with the channel radius, i.e., $\kappa_E = \partial E_{Sx}/\partial x = \partial E_{Sy}/\partial y$ and $\kappa_B = \partial B_{Sx}/\partial y = -\partial B_{Sy}/\partial x$, where $e\kappa_E = (1 - f)m_e \omega_p^2/2$ and $e\kappa_B = f m_e \omega_p^2 v_z/2c^2$. Substituting the static fields into Eqs.(1-4), one can have

$$\frac{dp_x}{dt} = -e\eta E_0 \cos(\phi) - e(\kappa_E + v_z \kappa_B)x, \quad (5)$$

$$\frac{dp_y}{dt} = -e(\kappa_E + v_z \kappa_B)y, \quad (6)$$

$$\frac{dp_z}{dt} = -ev_x E_0 \cos(\phi)/v_{ph} + e\kappa_B(v_x x + v_y y), \quad (7)$$

$$m_e c^2 \frac{d\gamma}{dt} = -ev_x E_0 \cos(\phi) - e\kappa_E(v_x x + v_y y). \quad (8)$$

These equations are not completely independent. From Eqs.(7) and (8) the integral of motion for the electron moving in this plasma channel can be expressed as $I \equiv \gamma m_e c^2 - v_{ph} p_z + e(\kappa_E + v_{ph} \kappa_B)r^2/2$, where $r^2 = x^2 + y^2$, and I is a constant decided by the initial condition of the electron. By employing this parameter, the four coupled equations can be reduced to three coupled equations.

In addition, in order to satisfy the resonance condition, electrons should be pre-accelerated to a relativistic energy [21]. One can mainly focus on the resonant electrons which will have $v \approx c$ and travel close to the channel axis. In this case, v_z is a slow variable compared with the fast variables of x and p_x . Thus one can further assume that $\kappa = e(\kappa_E + v_z \kappa_B)$ and $\eta = 1 - v_z/v_{ph}$ keep as constants in a suitable timescale. By taking the second derivative of the transverse momentum, Eqs.(5),(6), and (8) can be

written as

$$\frac{d^2 p_x}{dt^2} + \omega_\beta^2 p_x = m_e c a_0 \omega_L^2 \sin(\omega_L t), \quad (9)$$

$$\frac{d^2 p_y}{dt^2} + \omega_\beta^2 p_y = 0, \quad (10)$$

$$\gamma \frac{d\gamma}{dt} = -\omega_0 p_x a_0 \cos(\omega_L t) / m_e c, \quad (11)$$

where $\omega_\beta = \sqrt{\kappa/\gamma m_e}$ is the betatron frequency, $a_0 = eE_0/m_e \omega_0 c$ is the normalized amplitude of the laser field, and $\omega_L = \eta \omega_0$ is the laser frequency in the frame moving with the electron. Here the last two terms in Eq.(4) are neglected. It is noted that $\kappa = (1-f)m_e \omega_p^2/2 + f m_e \omega_p^2 v_z^2/2c^2 \approx m_e \omega_p^2/2$, which is not affected by the exact value of f . Then the betatron frequency can be expressed as $\omega_\beta \approx \omega_p/\sqrt{2\gamma}$. In the presence of a linearly polarized laser field, the electron would be preferentially accelerated along the laser polarization direction. Only Eq.(9) and Eq.(11) are coupled with each other when the initial condition is $p_y(t=0) = 0$. Thus the full equations can be reduced into the electron equation of motion along the laser polarization direction coupled with the energy equation. One can further employ the dimensionless variables with $\tau = \omega_L t$, $G = 2\gamma \frac{\omega_L^2}{\omega_p^2}$, $A_0 = 2a_0 \frac{\omega_L^2}{\omega_p^2 \sqrt{\eta}}$, and $P = 2 \frac{p_x}{m_e c} \frac{\omega_L^2}{\omega_p^2 \sqrt{\eta}}$. In these variables, the two coupled equations (9) and (11) can be rewritten as

$$\frac{d^2 P}{d\tau^2} + \frac{P}{G} = A_0 \sin(\tau), \quad (12)$$

$$G \frac{dG}{d\tau} = -P A_0 \cos(\tau). \quad (13)$$

It is noted that in this case the electron equation of motion is in the form of a parametric oscillator and the electron dynamics in the plasma channel only depend on two dimensionless parameters: $A_0 = 2a_0 \frac{\omega_L^2}{\omega_p^2 \sqrt{\eta}}$, and the initial Lorentz factor of the electron, $G_0 = 2\gamma_0 \omega_L^2/\omega_p^2 = \omega_L^2/\omega_{\beta 0}^2$. Here $\omega_{\beta 0} = \omega_p/\sqrt{2\gamma_0}$ refers to the initial betatron frequency and G_0 indicates the frequency deviation from the resonance condition.

For an ultra-intense laser pulse propagating into the under-dense plasma, the laser pulse is subject to wave dispersion and its phase velocity v_{ph} would be larger than c . The expression of v_{ph} was first given by Akhiezer and Polovin [29] for both linearly and circularly polarized laser pulse. In a travelling plane wave approach, it can be summarized as [29–31]

$$v_{ph} = c / \sqrt{1 - \frac{\omega_p^2}{\gamma_L \omega_0^2}}, \quad (14)$$

where $\gamma_L = \sqrt{1 + a_0^2/2} \approx a_0/\sqrt{2}$ refers to the averaged Lorentz factor of background plasmas. In this case, one has $v_{ph}/c \approx 1 + \frac{n}{\sqrt{2}a_0}$, thus $\eta = 1 - v_z/v_{ph} \approx n/\sqrt{2}a_0$ and $A_0 \approx \sqrt{\sqrt{2}n/a_0}$, where $n = \omega_p^2/\omega_0^2 = n_e/n_c$ is the

normalized plasma density and n_c is the critical plasma density. This shows that the electron dynamics is strongly dependent on a self-similar parameter of n/a_0 [32]. In another way, one can consider the plasma channel as a cylindrical waveguide, which also causes the wave dispersion for the laser pulse [26]. In this case, the phase velocity of the lowest mode in the plasma channel can be estimated as

$$v_{ph} = c / \sqrt{1 - \left(\frac{\lambda u_0}{2\pi R} \right)^2}, \quad (15)$$

where u_0 is the solution of $J_0(u) = 0$, J_0 refers to the zeroth-order Bessel function, and R denotes the radius of the plasma channel. For ultra-intense laser pulse propagating into the underdense plasmas, it will self-focus into the corresponding eigenmode with a beam radius of $2\sqrt{a_0}c/\omega_p$ [35]. By considering $R = 2\sqrt{a_0}c/\omega_p$ and $u_0 = 2.405$, then Eq.(15) can be written as $v_{ph} \approx 1 + \alpha \frac{n}{\sqrt{2}a_0}$, where $\alpha = u_0^2/4\sqrt{2} = 1.02$. It is shown that this kind of expression of v_{ph} is same with that in Eq.(14), which is only dependent on the single parameter of n/a_0 . This clearly indicates that the electron dynamics is characterized by the parameter of n/a_0 , which is also verified by our recent particle-in-cell simulation results [15]. In addition, it is noted that this parameter is completely different from previous works, in which the wave dispersion effect is not considered and it was shown that the parametric resonance is determined by the parameter of $a_0\sqrt{n}$ [22, 25]. Once the parameter n/a_0 is set as zero, Eqs.(12-13) would be reduced into the electron equation of motion in vacuum by interacting with a strong laser pulse. This indicates that our physical model can self-consistently describe the electron dynamics in a plasma channel.

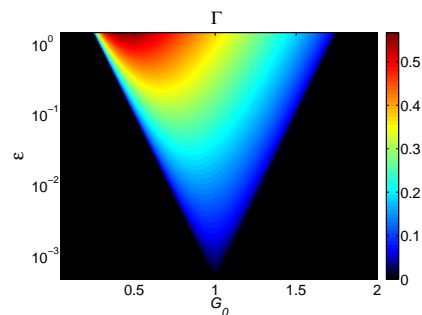


FIG. 1. (Color online) The phase space of the growth rate of the parametric instability.

The reduced model (Eqs.(12-13)) reveals the scheme of electron acceleration. However the nonlinearity appears to prevent one obtaining an analytical solution to Eqs.(12-13). The solution of Eq.(12) can be written as $P(\tau) = \varphi(\tau) \sin(\tau)$ with the initial condition of $P(\tau=0) = 0$, where $\varphi(\tau)$ is slowly varying amplitude. Substituting this solution into Eq.(13), one has

$G(\tau) = \sqrt{G_0^2 - 2A_0 \int \varphi(\tau) \sin(\tau) \cos(\tau) d\tau}$. This indicates that the Lorentz factor would be modulated by an oscillating term with twice the laser frequency [19, 20]. For the resonant electrons, one can assume that the variation of $G(\tau)$ relative to its initial value G_0 is negligible, then the solution of Eq.(13) can be approximately expressed as: $G(\tau) \approx G_0 - \delta G \cos(2\tau)$, where $\delta G \approx \frac{\bar{\varphi}(\tau)}{4G_0} A_0$ is the modulation amplitude and $\bar{\varphi}(\tau) = \int \varphi d\tau / \int d\tau$ is the averaged value of φ . Inserting $G(\tau)$ into Eq.(12) reduces it to a Mathieu equation [33] with an external driving force:

$$\frac{d^2 P}{d\tau^2} + \omega_G^2 (1 + \varepsilon \cos(2\tau)) P = A_0 \sin(\tau), \quad (16)$$

where $\omega_G^2 = \frac{1}{G_0}$ is the natural frequency and $\varepsilon = \frac{\delta G}{G_0}$ refers to the modulation amplitude of the natural frequency. The above equation can be further simplified as the classical Mathieu equation for $A_0 = 0$. In principle, the classical Mathieu equation allows for many unstable zones. In the presence of an external driven laser field, the electron would mainly execute the oscillation with the laser frequency. Thus, only the unstable solution around the fundamental resonance frequency is considered here. Substituting $P(\tau) = \varphi(\tau) \sin(\tau)$ into the reduced equation (13) yields $\varphi''(\tau) + \frac{[(1-\omega_G^2)^2 - (\omega_G^2 \varepsilon)^2/4]}{4} \varphi(\tau) + \frac{[(1-\omega_G^2) - (\omega_G^2 \varepsilon)/2]}{4} A_0 = 0$. It is clearly shown that there exists an exponentially growing solution in the form of $\exp(\Gamma\tau)$ when $(1-\omega_G^2)^2 < (\omega_G^2 \varepsilon)^2/4$ and the corresponding growth rate is

$$\Gamma = \sqrt{(\omega_G^2 \varepsilon)^2/4 - (1 - \omega_G^2)^2}/2. \quad (17)$$

It is noted that when the modulation amplitude $\varepsilon = 0$ or the modulation frequency is not twice the laser frequency, this kind of instability can never occur. Once the parametric modulation is ignored, Eq. (16) is reduced into the form of a forced oscillator, for which the solution in resonance can be expressed as $P(\tau) \approx \frac{A_0}{2\omega_G} \tau \sin(\tau)$ when $\omega_G \approx 1$ [24]. This shows that for the classical resonance the electron transverse momentum grows linearly with time and the averaged growth rate scales as $\frac{p_x(t)}{a_0 m_e c t} = \frac{P(\tau) \omega_L}{A_0 \tau} \propto \eta \propto \frac{n}{a_0}$.

From Eq. (17) one can elucidate some characteristics of the parametric resonance. The growth rate reaches its maximum value with $\Gamma_{max} = \frac{\varepsilon/4}{\sqrt{1-\varepsilon^2/4}}$ when $\omega_G^2 = \frac{1}{G_0} = \frac{1}{1-\varepsilon^2/4}$, and it corresponds to the resonance in fundamental frequency. The width of the resonance region is determined by the inequality $|1 - \omega_G^2| < \omega_G^2 \varepsilon/2$ and it also depends on the modulation amplitude ε . It is shown from Fig. 1 that the parametric resonance is restricted in a special tongue-shaped region and the growth rate of the instability, the width of resonance region, as well as the resonance frequency will all increase with the modulation amplitude ($\varepsilon \approx \frac{\bar{\varphi} A_0}{4G_0^2}$), which is proportional to the strength of the driving force (A_0). However, as the

electron is accelerated by the laser pulse, the growth of the Lorentz factor will shift the electron out of resonance, and lead to a reduction on the growth rate of parametric resonance. In addition, it is noted that the damping rate ($\beta = \frac{dG/d\tau}{2G} \propto \Gamma \propto \varepsilon \propto A_0$) is proportional to the value of A_0 . Therefore, the damping effect will gradually play an important role with the increase of A_0 . That is, the resonance efficiency will be reduced and even the typical resonance peak will gradually disappear with the increase of A_0 . It is implied that the parametric resonance may take place and dominate the electron acceleration process for a relatively small parameter of n/a_0 .

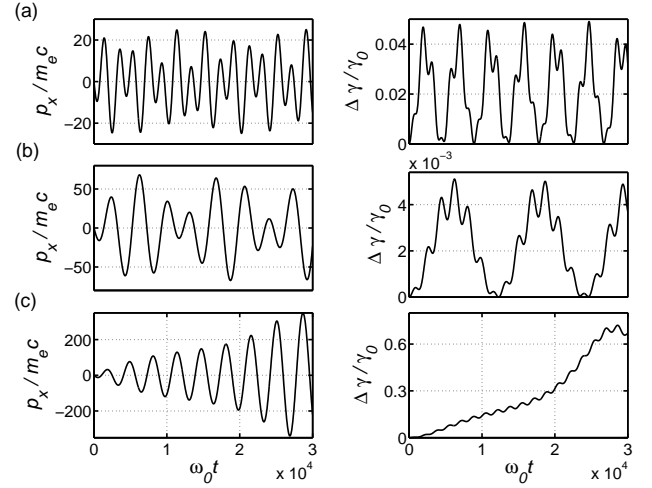


FIG. 2. The numerical solutions of Eqs.(1-4). (a-c) The time evolutions of the transverse momentum ($p_x/m_e c$) and the energy gain ($\Delta\gamma/\gamma_0 \equiv (\gamma_{max} - \gamma_0)/\gamma_0$) of the electron for different initial energies. The initial parameters are $n/a_0 = 0.0025$ and $a_0 = 20$, and the initial conditions are $\vec{r}(0) = 0$, $p_x(0) = 0$, $p_y(0) = 0$, and $p_z(0) = \sqrt{\gamma_0^2 - 1}$, where (a), (b), and (c) respectively correspond to $\gamma_0 = 0.3a_0^2/n$, $\gamma_0 = 2a_0^2/n$, and $\gamma_0 = 0.66a_0^2/n$.

III. NUMERICAL SIMULATIONS

In order to test the theoretical predictions, numerical simulations based on Eqs.(1-4), along with $d\vec{r}/dt = \vec{p}/\gamma m_e$, are carried out by employing the fourth-order Runge-Kutta method [34]. Fig. 2 shows the non-resonant and resonant solutions of the electron motion at different initial energies for $n/a_0 = 0.0025$. The parametric resonance occurs when the modulation frequency ($\omega_m = 2\omega_L$) is about twice the betatron frequency. This gives the resonance condition as $G_0 \approx 1$, i.e., $\omega_{\beta 0} \approx \omega_m/2 = \eta\omega_0 \approx \omega_0 n/\sqrt{2}a_0$. From this one can obtain the initial electron energy that is required to meet the resonance condition is about $\gamma_0 \approx a_0^2/n$. It is shown from Fig. 2(a) and (b) that when the initial electron energy is deviated from the value of a_0^2/n , the electron motion displays randomly modulated behavior and the energy

gain is negligible. However, when the initial electron energy is close to the value of a_0^2/n , the modulation frequency gets close to twice the betatron frequency. In this case, the electron can resonantly interact with the laser field and the electron energy can be largely enhanced. Fig. 2(c) shows that for the resonant electron its energy experiences a nonlinear growing process and the energy gain is significant. The dependence of the resonance behavior on the initial electron energy is clearly shown in Fig. 3. This indicates that there exists a sharp boundary above which the resonance behavior can be excited and the resonance only occurs in a restricted region, which agrees well with the characteristics of the parametric resonance shown in Fig. 1.

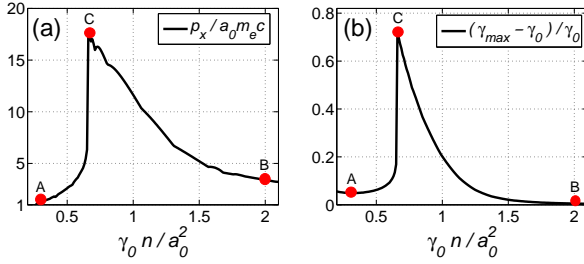


FIG. 3. The resonance peaks of the maximum transverse momentum $p_{x,max}/a_0 m_e c$ (a) and the maximum energy gain $(\gamma_{max} - \gamma_0)/\gamma_0$ (b) of the electron for different γ_0 , where $p_{x,max}$ refers to the maximum value of p_x and γ_{max} is the maximum Lorentz factor. The labelled points A, B, and C respectively correspond to the solutions in Fig. 2.

Fig. 4 shows one typical resonant solution for $n/a_0 = 0.0025$. This shows that when the betatron frequency of the electron is close to half of the modulation frequency with $\omega_\beta = 0.57\omega_m$, both the electron transverse momentum and energy experience a nonlinear growing process, as shown in Figs. 4(a) and (c). In this case, Fig. 4(a) shows that the electron can stay in phase with the witnessed laser field until the dephasing occurs, ensuring that the electron can continuously gain energy from the laser pulse. The expanding spacing of different trajectories in the phase space shown in Fig. 4(b) indicates that this kind of resonance is a nonlinear process. In addition, it is noted from Fig. 4(c) that the growing Lorentz factor is accompanied by a modulation with twice the laser frequency. The Lorentz factor can be separated as $\gamma(t)/\gamma_0 = \gamma_d(t) + \delta\gamma(t)$, where γ_d refers to the non-oscillating term and reveals the growth of electron energy, $\delta\gamma(t)$ is the oscillating term and $\varepsilon = \delta\gamma/\gamma_d$ denotes the modulation amplitude. Fig. 4(c) shows that the modulation amplitude increases with the transverse momentum. Such a twice frequency modulation is a necessary condition to excite the nonlinear parametric resonance. Fig. 4(d) shows that for the resonant electrons the longitudinal velocity v_z is a slow variable compared with the fast variables of x and p_x , suggesting that our assumptions are reasonable and the reduced model (Eqs.(12-13)) can reveal the scheme of electron acceleration.

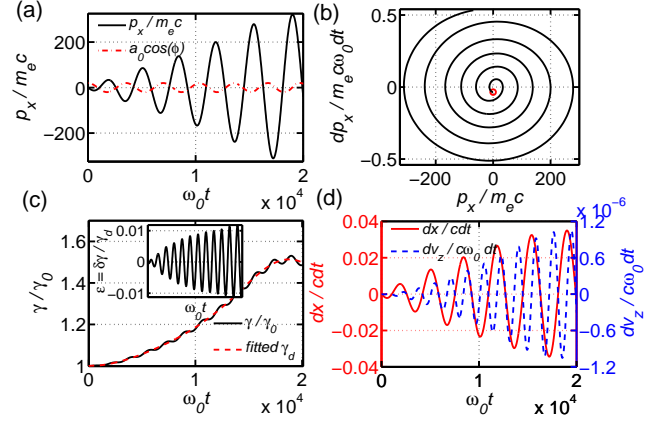


FIG. 4. (Color online) A typical resonant solution of Eqs.(1-4). (a) The time evolution of the electron transverse momentum, where the red curve is the laser field witnessed by the electron; (b) The corresponding phase space of (a) and the red circle shows its initial position; (c) The time evolution of the Lorentz factor of the electron, where the red line shows the fitted curve of the non-oscillating term and the inset shows the evolution of the oscillating term; (d) The time evolution of the derivative of the fast variable x and the slow variable v_z . The initial parameters are $n/a_0 = 0.0025$, $a_0 = 20$, and $\gamma_0 = 0.75a_0^2/n$, and the initial conditions are $\vec{r}(0) = 0$, $p_x(0) = 0$, $p_y(0) = 0$, and $p_z(0) = \sqrt{\gamma_0^2 - 1}$.

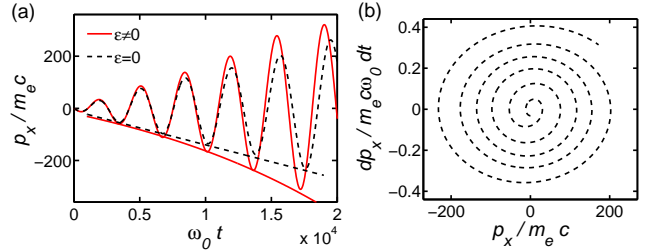


FIG. 5. (Color online) (a) The time evolutions of electron transverse momentum, where the red solid curve corresponds to the solution of Eqs.(1-4) and the black dashed curve is the corresponding solution obtained by neglecting the oscillating term in the Lorentz factor shown in Fig. 4(c) and substituting the non-oscillating term $\gamma_d(t)$ into Eq.(9). (b) The corresponding phase space of the black dashed curve in (a). The initial parameters are same with that in Fig. 4. The envelopes of electron transverse momentum in (a) respectively correspond to the fitted solutions of $p_x(t)/m_e c = 200 \times [1 - \exp(5.4 \times 10^{-5} \omega_0 t)]$ (red solid curve) and $p_x(t)/m_e c = -0.013 \omega_0 t$ (black dashed curve).

To clearly illustrate the parametric resonance behavior, Fig. 5(a) shows the resonant solution excluding the parametric modulation, which is given by substituting the non-oscillating term of the Lorentz factor ($\gamma_d(t)$) in Fig. 4(c) into Eq.(9). It is shown that the electron transverse momentum grows linearly with time and the spacing of different trajectories in phase space is almost the same, as shown in Fig. 5(b). Particularly, it is noted

from Fig. 5(a) that when the modulation term of the Lorentz factor is included, the electron transverse momentum grows exponentially with time in the form of $p_x(t)/m_e c \approx 200 \times [1 - \exp(5.4 \times 10^{-5} \omega_0 t)]$. This clearly indicates that the parametric resonance is excited by the twice frequency modulation. In this case, the electron transverse momentum grows faster than that in classical linear resonance regime.

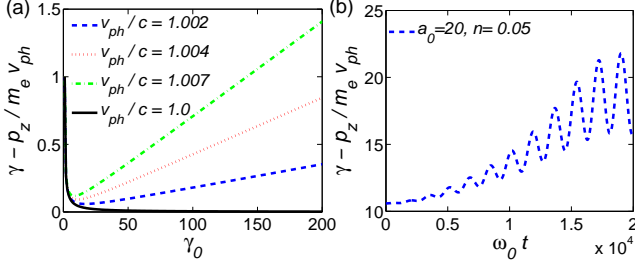


FIG. 6. (Color online) (a) The dephasing rate as a function of the initial Lorentz factor for different phase velocities; (b) The time evolution of the dephasing rate, which corresponds to the solution shown in Fig. 4.

The electron can only be accelerated when it stays in phase with the laser field, as shown in Fig. 4(a). However, the dephasing between the electron and the laser field gradually occurs when the electron is further accelerated. The dephasing rate can be expressed as $R = \gamma \frac{d\phi}{dt} = \gamma - \frac{p_z}{m_e v_{ph}}$. It is noted that this is different from that considered in previous works [22, 25], where the phase velocity of the laser pulse is equal to c . Fig. 6(a) shows that even a slight difference between the phase velocity of the laser pulse, v_{ph} , and the light speed in vacuum, c , would affect the dephasing rate significantly. For the case of $v_{ph} = c$, the dephasing rate is decreased when the electron is accelerated. However, for the case of $v_{ph} > c$, the dephasing rate would increase with the electron energy when the initial electron energy is large enough. Fig. 6(b) shows the time evolution of the dephasing rate, which corresponds to the solution shown in Fig. 4. It is shown that with the acceleration of the electron, its dephasing rate is also increased. But in this case, the laser phase witnessed by the resonant electrons changes slowly so that the electron can still stay in phase with the laser pulse for a long time until the dephasing occurs.

Fig. 7 shows the phase space of the maximum momentum and Lorentz factor of the electron for different initial parameters. It is clearly shown that a special tongue-shaped structure exists around the resonance point when the value of A_0 is relatively small. This is a signature of parametric resonance [33], as demonstrated in Fig. 1. This special structure is also reproduced by directly solving the Eqs.(1-4), as shown in Figs. 7(c) and (d). In addition, it is indicated that the parametric resonance is strongly dependent on the self-similar parameter of n/a_0 , which agrees well with the theoretical predictions.

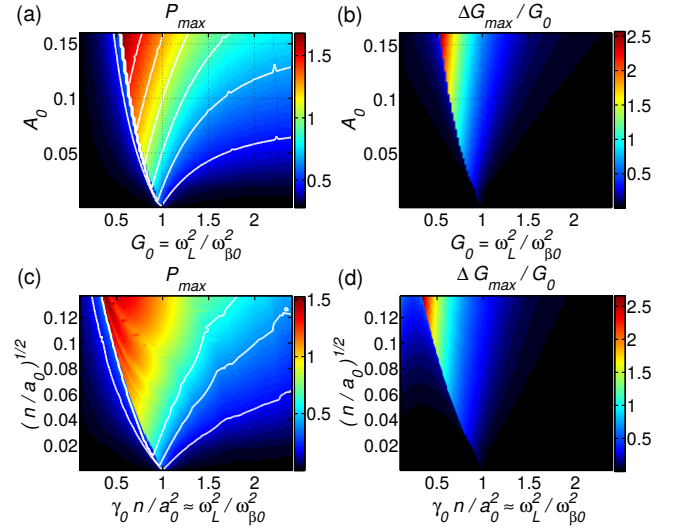


FIG. 7. (Color online) [(a) and (c)] The phase spaces of the maximum electron momentum P_{max} along the laser polarization direction. [(b) and (d)] The phase spaces of the increase of Lorentz factor of the electron ($\Delta G_{max} = G_{max} - G_0$). G_0 refers to the initial normalized Lorentz factor of the electron and A_0 denotes the amplitude of the driving force in Eq.(12). The results in (a) and (b) are computed from Eqs.(12-13) and the initial conditions are set as $P(0) = 0$ and $P'(0) = 0$. The results in (c) and (d) are computed from Eqs.(1-4) and the initial conditions are $a_0 = 10$, $\vec{r}(0) = 0$, $p_x(0) = 0$, $p_y(0) = 0$, and $p_z(0) = \sqrt{\gamma_0^2 - 1}$. The white lines in (a) and (c) are the corresponding contour plots.

For clarity, the resonance behavior is also shown in Fig. 8. To clearly demonstrate the resonance efficiency, one can further define a quality factor of the parametric resonance as $Q = \frac{p_x}{a_0 m_e c}$. As is well known, for an electron interacted with a laser pulse in vacuum, the maximum value of Q is always equal to unity regardless of its initial condition [25]. However, in a plasma channel, the Q factor can be greatly amplified by the parametric resonance process, as shown in Fig. 8(a). Fig. 8(f) shows that the modulation amplitude is proportional to the value of n/a_0 . Correspondingly, as predicted by the theory, with the increase of n/a_0 the growth rate of the instability is increased, the width of resonance region is expanded, but the resonance efficiency is much reduced, as shown in Fig. 8(e). To ascertain the boundary value of n/a_0 for efficient parametric resonance, one can assume that when the width of resonance region is on the same order of the resonance frequency, i.e., $\Delta G_0 \sim G_r \sim 1$, the parametric resonance would lose its efficacy. This gives a boundary value of $n/a_0 = 0.068$, as demonstrated in Fig. 8(e), in this case it can be seen from Figs. 8(a) and (b) that even the typical resonance peak is gradually disappeared.

Figs. 8(c) and (d) show that for a fixed value of n/a_0 the maximum transverse momentum and the energy gain of the electron grow linearly with a_0 , suggesting that the Q factor and the normalized energy gain $((\gamma_{max} - \gamma_0)/a_0)$ are self-similar parameters and only depend on the val-

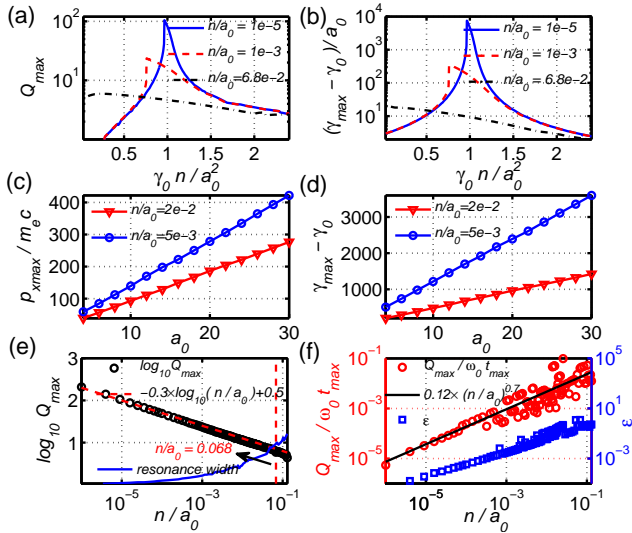


FIG. 8. (Color online) The resonance peaks of the quality factor $Q_{max} = p_{xmax}/a_0 m_e c$ (a) and energy gain $(\gamma_{max} - \gamma_0)$ (b) of the electron for different n/a_0 , respectively. The scalings of $p_{xmax}/m_e c$ (c) and $(\gamma_{max} - \gamma_0)$ (d) with a_0 for different fixed values of n/a_0 . (e) The amplitude (circles) and the resonance width of Q_{max} is calculated at $1/\sqrt{2}$ of the maximum value of the resonance peak. The averaged growth rate of Q (red circles) and the modulation amplitude of the Lorentz factor ϵ (blue squares) are depicted in (f), where t_{max} refers to the acceleration time and scales as $\omega_0 t_{max} \propto (n/a_0)^{-1}$. The initial conditions are same as that in Figs. 7(c) and (d).

ue of n/a_0 . For the parametric resonance, the resonance behavior is restricted in a special region and the resonance efficiency decreases when the resonance width is expanded. This is similar to the classical resonance, but essentially, it is different from the classical resonance behavior because it manifests the instability phenomenon. In addition, it is noted that the averaged growth rate of electron transverse momentum in this case scales as $Q(t)/t \propto (n/a_0)^{0.7}$, as shown in Fig. 8(f), which indicates that the electron transverse momentum in the nonlinear parametric resonance regime grows faster than that in the linear classical resonance regime ($Q(t)/t \propto n/a_0$) for $n/a_0 \ll 1$.

IV. DISCUSSIONS

In the above simulations, a plane wave is considered for simplicity, which is valid for a wide laser beam. In the realistic case, when the radial excursion of electron becomes comparable with the laser beam size, the radial nonuniformity of the laser field would affect the parametric resonance process. It is noted that for ultra-intense laser pulse propagating in the underdense plasmas, when the laser beam radius (r_0) is about twice the relativistically-corrected plasma skin depth $2\sqrt{a_0}c/\omega_p$, the laser beam

can match well with the plasma and stably propagate into the plasma [35–37]. For the electron interacting with a laser pulse with a finite beam size of $r_0 = 2\sqrt{a_0}c/\omega_p$, the corresponding simulation result is shown in Fig. 9. This shows that with the increase of transverse excursion of the electron, the nonuniformity of the laser field would gradually take effect and result in the reduction of the Lorentz factor and electron transverse momentum. When the electron deviates from the central region, it experiences a weaker laser field and the laser frequency in the electron frame is continuously changed, as a result, the Lorentz factor of the electron is randomly modulated [20], as shown in Fig. 9(b). In this case, the modulation frequency can not match with the betatron frequency of the electron motion and the parametric resonance gradually loses its efficacy. Fig. 9(a) shows that the electron transverse momentum first experiences an exponentially growing process then degrades into a linearly growing process. Thus, when the electron excursion is relatively small, the nonuniformity of the laser field does not affect the electron motion significantly and parametric resonance can still be excited for a long time.

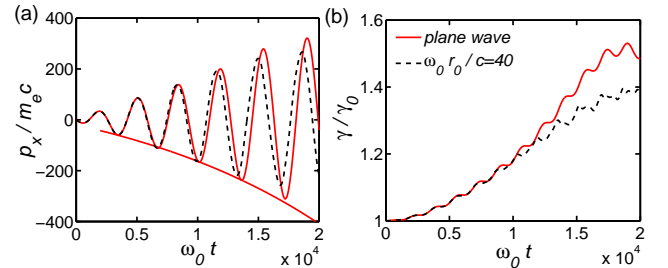


FIG. 9. (Color online) (a) The time evolutions of the electron transverse momentum for different beam radiuses, where the red solid line corresponds to the plane wave and the blue dashed line corresponds to the Gaussian laser with a beam radius of $r_0 = 2\sqrt{a_0}c/\omega_p$ ($\omega_0 r_0/c = 2\sqrt{a_0/n_e/n_c} = 40$). (b) The corresponding time evolutions of the Lorentz factor for different beam radiuses. The fitted curve in (a) corresponds to the solution of $p_x(t)/m_e c = 200 \times [1 - \exp(5.4 \times 10^{-5} \omega_0 t)]$. The simulation parameters are the same with that in Fig. 4.

By exploiting the nonlinear parametric resonance process, it is possible to enormously amplify the energy and transverse momentum of the electron by employing a relatively small value of n/a_0 . This could be beneficial to the generation of high-flux and high energy radiation sources because an extremely large betatron strength ($a_\beta = \gamma r_\beta \omega_\beta/c$) parameter, which also represents the electron transverse momentum, can be achieved in this regime. Here r_β refers to the transverse betatron amplitude. However, it is noted that to observe the parametric resonance behavior or to get an efficient amplification of the energy and transverse momentum of the electron, the electron must be pre-accelerated to a high energy with $\gamma_0 \approx \alpha a_0^2/n$ to meet the resonance condition, here $\alpha \approx 1 - 2.45(n/a_0)^{1/3}$ ($0 < \alpha < 1$) represents

the resonance point in Fig. 7. In the simulations and experiments, the longitudinal charge separation electric field [12, 23, 37] and the surface electric field [38, 39] can be an external force to pre-accelerate the electrons. Nevertheless, when the value of n/a_0 is very small, the pre-acceleration would become a critical problem. In addition, the electron acceleration is limited by the dephasing between the electron and the laser field. It is noted from Fig. 8 that the acceleration time for the resonant electron ($T_{acc} \approx 4.2 \frac{a_0}{n} T_L$) is inversely proportional to the value of $\frac{n}{a_0}$ [15]. That is, for a very small value of n/a_0 , the long distance propagation for the laser pulse in underdense plasmas is required for efficient electron acceleration, which would also become a crucial problem. Therefore, in order to realize parametric resonance in the laboratory, a relatively large value of n/a_0 can be chosen. In this case, the pre-acceleration can be easily achieved at the expense of decreasing the resonance efficiency.

V. SUMMARY

In summary, we have studied the role of nonlinear parametric resonance in direct laser acceleration. Based on the single particle model that incorporates the wave dispersion relation, it is shown that the region of parametric resonance is decided by a single parameter of n/a_0 . Numerical simulations indicate that when the parameter n/a_0 is small ($n/a_0 < 0.068$), the parametric resonance can become the dominant process for high energy electrons. With the decrease of n/a_0 the width of the reso-

nance region is decreased but the resonance efficiency is much enhanced. However, for a small value of n/a_0 , a high initial electron energy and a long interaction length is required to get an efficient energy gain. It is suggested that a relatively large value of n/a_0 can be chosen to achieve the parametric resonance in a laboratory at the expense of decreasing the resonance efficiency. By exploiting this regime it may be easier to reach high electron energies and transverse momenta which are important for optimising X-ray production from laser-plasma sources.

VI. ACKNOWLEDGEMENTS

This work is supported by the National Key Programme for S&T Research and Development, Grant No. 2016YFA0401100, the National Natural Science Foundation of China (NSFC), Grants No. 11575298, No. 91230205, No. 11575031, and No. 11175026, the National Basic Research 973 Project, No. 2013CB834100, the NSAF, Grant No. U1630246, and the National High-Tech 863 Project. B. Q. acknowledges the support from Thousand Young Talents Program of China. T. W. H. acknowledges the support from China Scholarship Council. We would like to thank Robbie Scott, Holger Schmitz and Raoul Trines for their useful discussions and help. T. W. H. would also like to thank Naren Ratan, Luke Ceurvorst, Muhammad Kasim, James Sadler, Jimmy Holloway, and Matthew Levy at Oxford University for their help and guidance in this work.

-
- [1] S. P. D. Mangles *et al.*, Nature (London) **431**, 535 (2004).
 - [2] C. G. R. Geddes *et al.*, Nature (London) **431**, 538 (2004).
 - [3] J. Faure *et al.*, Nature (London) **431**, 541 (2004).
 - [4] P. A. Norreys, Nat. Photonics **3**, 423 (2009).
 - [5] E. Esarey, C. B. Schroeder, and W. P. Leemans, Rev. Mod. Phys. **81**, 1229 (2009).
 - [6] H. Chen *et al.*, Phys. Rev. Lett. **105**, 015003 (2010).
 - [7] S. Corde *et al.*, Rev. Mod. Phys. **85**, 1 (2013).
 - [8] K. Ta Phuoc *et al.*, Phys. Plasmas **12**, 023101 (2005).
 - [9] E. Esarey *et al.*, Phys. Rev. **E65**, 056505 (2002).
 - [10] S. Kiselev, A. Pukhov, and I. Kostyukov, Phys. Rev. Lett. **93**, 135004 (2004).
 - [11] A. Rousse *et al.*, Phys. Rev. Lett. **93**, 135005 (2004).
 - [12] S. Cipiccia *et al.*, Nat. Phys **7**, 867 (2011).
 - [13] S. Kneip *et al.*, Phys. Rev. Lett. **100**, 105006 (2008); S. Kneip *et al.*, Proc. SPIE **7359**, 73590T (2009).
 - [14] B. Liu *et al.*, Phys. Plasmas **22**, 080704 (2015).
 - [15] T. W. Huang *et al.*, Phys. Rev. **E93**, 063203 (2016).
 - [16] C. Gahn *et al.*, Phys. Rev. Lett. **83**, 4772 (1999).
 - [17] G. D. Tsakiris, C. Gahn, and V. K. Tripathi, Phys. Plasmas **7**, 3017 (2000).
 - [18] S. P. D. Mangles *et al.*, Phys. Rev. Lett. **94**, 245001 (2005).
 - [19] A. Pukhov, Z. M. Sheng, and J. Meyer-ter-Vehn, Phys. Plasmas **6**, 2847 (1999).
 - [20] B. Qiao *et al.*, Phys. Plasmas **12**, 083102 (2005); H. Y. Niu *et al.*, Laser Part. Beams **26**, 51 (2008).
 - [21] B. Liu *et al.*, Phys. Rev. Lett. **110**, 045002 (2013).
 - [22] A. V. Arefiev *et al.*, Journal of Plasma Physics, **81**, 475810404 (2015).
 - [23] A. P. L. Robinson, A. V. Arefiev, and D. Neely, Phys. Rev. Lett. **111**, 065002 (2013).
 - [24] L. D. Landau and E. M. Lifshitz, *Mechanics: Volume 1 of Course of Theoretical Physics* (Elsevier, Oxford, 1976), pp.58-87.
 - [25] A. V. Arefiev *et al.*, Phys. Rev. Lett. **108**, 145004 (2012); A. V. Arefiev, V. N. Khudik, and M. Schollmeier, Phys. Plasmas **21**, 033104 (2014); A. V. Arefiev *et al.*, Phys. Plasmas **23**, 023111 (2016); A. V. Arefiev *et al.*, Phys. Plasmas **23**, 056704 (2016).
 - [26] A. P. L. Robinson, A. V. Arefiev, and V. N. Khudik, Phys. Plasmas **22**, 083114 (2015).
 - [27] I. Kostyukov, A. Pukhov, and S. Kiselev, Phys. Plasmas **11**, 5256 (2004).
 - [28] W. Lu *et al.*, Phys. Plasmas **13**, 056709 (2006).
 - [29] A.I. Akhiezer and R.V. Polovin, Zh. Eksp. Teor. Fiz. **80**, 915 (1956) [Sov. Phys. JETP **8**, 696 (1956)].
 - [30] C. D. Decker and W. B. Mori, Phys. Rev. Lett. **72**, 490 (1994).
 - [31] R. H. Hu *et al.*, Sci. Reports, **5**, 15499 (2015).

- [32] S. Gordienko and A. Pukhov, Phys. Plasmas **12**, 043109 (2005).
- [33] V. I. Arnold, *Mathematical Methods of Classical Mechanics* (Springer-Verlag, New York, 1989), pp.113-122.
- [34] In the simulations, the value of f is assumed to be 1/2. The value of f actually does not affect the electron dynamics in the simulations, which can also be seen from the theoretical derivations. The phase velocity of the laser pulse is taken in the form of Eq.(14).
- [35] T. W. Huang, C. T. Zhou, and X. T. He, Laser Part. Beams **33**, 347 (2015); T. W. Huang *et al.*, Phys. Rev. **E** **92**, 053106 (2015).
- [36] G. Z. Sun *et al.*, Phys. Fluids **30**, 526 (1987).
- [37] W. Lu *et al.*, Phys. Rev. ST Accel. Beams **10**, 061301 (2007).
- [38] N. Naseri *et al.*, Phys. Rev. Lett. **108**, 105001 (2012).
- [39] L. Willingale *et al.*, Phys. Rev. Lett. **106**, 105002 (2011);